Catal Lett (2008) 126:78–83
DOI 10.1007/s10562-008-9561-y

Novel Silver Loaded Hydroxyapatite Catalyst for the Selective Catalytic Reduction of NO_x by Propene

Pullur Anil Kumar · Maddigapu Pratap Reddy · Lee Kyung Ju · Ha Heon Phil

Received: 31 January 2008 / Accepted: 27 June 2008 / Published online: 18 September 2008

Abstract A novel and high performance silver loaded hydroxyapatite (HAp) catalyst for the selective catalytic reduction (SCR) of NO_x by propene is reported for the first time. The catalysts with variable silver contents have been prepared and characterized extensively by different techniques such as XRD, XPS, BET-surface area, TPR, TPD and ICP analyses. The $DeNO_x$ activities of these catalysts are measured at reaction temperature ranged from 250 to 500 °C. The 1.5 wt.% Ag/HAp is found to be best among all the catalysts studied showing about 70% conversion and 60% selectivity towards N_2 formation at 375 °C in oxygen rich atmosphere.

Keywords Hydroxyapatite · Ag/HAp · Selective catalytic reduction of NO_x · NO_x conversion to N_2 · XPS · TPR

1 Introduction

Air pollution by nitrogen oxides (NO_x) is currently one of the most serious environmental problems. The conventional three-way catalyst shows low NO_x conversion in lean-burnt exhaust that contains high concentration of O_2. Awareness of this pollution control and the new stringent regulations on the emission levels of nitrogen oxides from transportation vehicles lead to a recent active research in the catalytic reduction of NO_x to N_2 with hydrocarbons. Metal-ion exchanged zeolites are among the most promising and more efficient at lower temperatures and lower oxygen partial pressures for $DeNO_x$ but failed under lean conditions and high temperatures. Alumina based catalysts are more attractive as they are hydrothermally stable. Many metal/metal oxides (In, Mn_3O_4, Mn, Co, CoO_x, Ag, Sn, Ga, Ga_2O_3, Cu, Au) supported on alumina have been synthesized by either sol-gel or incipient wetness impregnation methods and investigated for NO_x reduction [1–5]. The noble metal catalysts have shown high activity for this reaction, presenting NO_x conversion window at much lower temperatures than zeolite catalysts, however, they showed poor nitrogen selectivity [6].

Hydroxyapatite (HAp) is the major inorganic component in natural bones and can be synthesized by precipitation, solid-state reaction, hydrothermal method, sol-gel synthesis and other routes [7]. Owing to its unique acid-base properties, hydroxyapatite attracted much attention as solid catalyst more recently for various reactions such as dehydration and dehydrogenation of alcohols [8, 9], oxidation of alkanes [10, 11], Knoevenagel condensation [12], Friedel-Crafts alkylation [13], and Michael addition [14] and WGS reaction [15]. Hydroxyapatite is also used as a catalyst support for transition metal catalysts in various types of oxidation and carbon-carbon bond forming reactions [16].

Silver catalysts were known to be most effective materials for selective catalytic reduction (SCR) of NO_x in excess oxygen and were investigated intensively since 1990s [17–21]. Among the several supports for silver, g-Al_2O_3 is superior to TiO_2, SiO_2, ZrO_2, TiO_2–ZrO_2 and Ga_2O_3 [22–24]. Moreover, most of reports have already suggested that highly isolated Ag cations, strongly bonded to alumina, are the active sites for the selective catalytic reduction of NO_x [25], whereas metallic silver clusters dominate in the high silver content alumina-based

P. A. Kumar · M. P. Reddy · L. K. Ju · H. H. Phil (✉)
Advanced Functional Materials Research Center, Korea Institute of Science and Technology, Cheongryang, Seoul 130-650, Republic of Korea
e-mail: heonphil@kist.re.kr

catalysts, which are less selective for NO_x reduction and good for the direct combustion of hydrocarbons [26]. Much attention was paid by previous researchers to correlate the nature of Ag species with their catalytic behaviors and redox properties of the catalysts as mentioned in literature [19, 25, 27]. As the alumina surface –OH groups might contribute to Ag species being evenly dispersed, it is hoped that hydroxyapatite surface –OH groups also possible to contribute to Ag species evenly dispersion. Due to its redox properties, hydroxyapatite has been chosen for the first time as a catalyst support for selective catalytic reduction of NO_x.

In this communication, we report silver loaded hydroxyapatite catalyst prepared by simple wet impregnation method and $DeNO_x$ activities were measured using propene under oxygen rich atmosphere.

2 Experimental

2.1 Catalyst Preparation

The hydroxyapatite was prepared by conventional method as reported elsewhere [15, 28]. Different weight percentages of silver i.e., 0.5, 1.0, 1.5, 2 and 4 were loaded by incipient wet impregnation method using $AgNO_3$ as precursor and the loaded catalyst was dried and subsequently calcined at 600 °C for 4 h.

2.2 Characterization of Catalysts

The powder XRD patterns were measured on a Siemens 5000 X-ray diffractometer with Bruker D8 Advance having Cu Kα radiation ($\lambda = 1.5418$ A). X-ray photo electronic spectrographs (XPS) were recorded on a PHI 5800 ESCA system. The BET-surface area, H_2-TPR and NH_3-TPD patterns are measured by using Auto-Chem II chemisorption analyzer and ICP analysis was carried out by Perkin-Elmer ELAN DRC plus system.

2.3 Activity Measurements

Catalytic activity tests were performed in a dynamic online micro reactor using a feed stream consisting of 800 ppm NO_x, 800 ppm C_3H_6, 6% O_2, balance helium, with a total flow rate of 100 cc/min over 0.25 g catalyst. The effluent from the reactor was analyzed by an online NDIR Fuji NO analyzer and VARIAN Micro-GC 4900 using Poraplot-Q and Molecular Sieve 5A columns. The NO conversion and selectivity towards N_2 formation were calculated using the formulae $NO_x^{out}/NO_x^{in} \times 100$ and $2[N_2]/NO_x^{in} \times 100$ respectively.

3 Results and Discussion

3.1 XRD and BET-SA

Figure 1 shows the XRD patterns of HAp and silver loaded HAp catalysts. The peaks at $2\theta = 31.74$, 32.18 and 32.89 can be indexed to hydroxyapatite (JCPDS card No.24–33). Increasing silver weight percentage on HAp from 0.5 and 4 wt.%, peaks due to metallic silver appeared in higher loadings at $2\theta = 38.1$ and 44.2 (JCPDS card No. 4–783). The peaks due to Ag_2O appeared at $2\theta = 32.7$ (JCPDS card No. 6–505) in higher loading catalysts. In lower loadings the presence of Ag_2O (0.5–1.5%) phase is not observed due to high dispersion. Figure 2 represents the comparison of XRD patterns between fresh and used catalysts. The size of the corresponding silver crystal was estimated by the Scherrer procedure. The estimated silver crystallite sizes were given in the Table 1. The analysis of the peak at 2 theta 38.1° (Fig. 2) revealed the presence of bigger silver crystals in used catalysts compared to fresh catalysts after calcination [29]. A narrow peak accounted for a silver content of 1.5% Ag/Al_2O_3 and corresponded to a crystal size of 19 nm (Table. 1). This is significantly lower size of silver crystal compared to 4% Ag/HAP catalyst which shows 51 nm. Crystallite size was also calculated for the used catalysts after reaction and is shown in Table 1. Due to the sintering at higher temperatures of the used catalysts of higher loadings shows bigger crystallite sizes. BET-Surface areas and weight percentage of silver of all the samples were given in Table 2. It could be seen that the highest surface area is obtained for pure hydroxyapatite, the values decrease with progressive increase in loading of silver to the support which is expected.

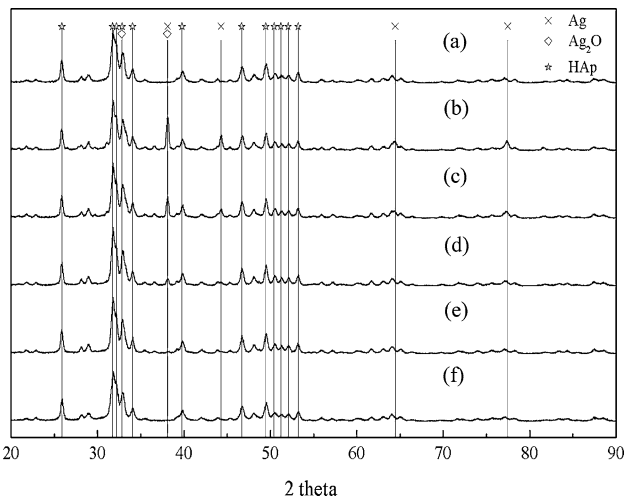

Fig. 1 X-ray diffraction Patterns of (a) HAp (b) 4% Ag/HAp (c) 2% Ag/HAp (d) 1.5% Ag/Hap (e) 1% Ag/HAp (f) 0.5% Ag/Hap

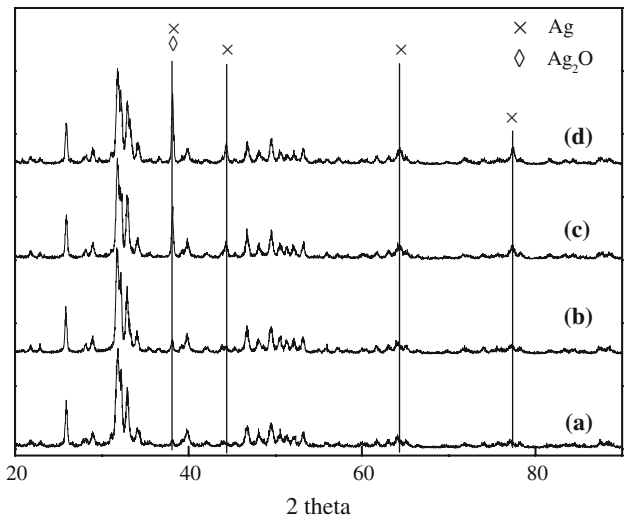

Fig. 2 X-ray diffraction Patterns of fresh and spent catalysts (a) Fresh—1% Ag/HAp (b) Spent—1% Ag/HAp (c) Fresh—4% Ag/HAp (d) spent—4% Ag/Hap

Table 1 Crystalline properties of silver observed in XRD patterns of fresh and used catalysts

Catalyst	Silver crystal size (nm)	
	Fresh	Spent
1.5% Ag/HAp	19	30
2.0% Ag/HAp	35	67
4.0% Ag/HAp	51	93

Table 2 ICP analysis and BET-surface area of the fresh catalysts

Catalyst	Wt.% of Ag (ICP)	BET-SA (m^2/g)
HAp	0.0	57
0.5% Ag/HAp	0.47	50
1.0% Ag/HAp	0.95	46
1.5% Ag/HAp	1.55	43
2.0% Ag/HAp	1.91	41
4.0% Ag/HAp	3.96	40

3.2 XPS

The XPS results of pure HAp and 1.5 wt.% Ag/HAp catalysts are shown in Fig. 3 A. The binding energy values of O1 s of hydroxide and phosphate are observed at 531.91 eV and 530.79 eV respectively (Fig. 3a (a)). In case of silver loaded HAp catalysts additional peak pertaining to silver oxide is also seen. In Fig. 3a (b) XPS spectrum of 1.5% Ag/HAp catalyst an additional Ag_2O peak at the binding energy of 529.27 eV is observed, confirming the presence of silver dispersion over HAp. The typical XPS for Ag 3d in all silver loadings (Fig. 3b) showed two peaks at the binding energies of 368.3 eV and 367.8 eV corresponding to metallic silver and silver oxide respectively [30].

3.3 NH_3-TPD and TPR

Acidity measurements of all samples are carried out by NH_3-TPD experiment using 5% NH_3/He gas (Table 3) from RT to 600 °C. The T_{max} was decreased with the increasing silver loading from 0.5 to 4 wt.% and total acidity also decreased with increasing Ag loading on HAp. Figure 3 shows the H_2-TPR patterns of all calcined samples of HAp and Ag/HAp, which showed no reduction peak for HAp. TPR profiles of all Ag/HAp catalysts showed one reduction peak in whole temperature range, which can be attributed to silver oxide reduction. In Table 3 hydrogen

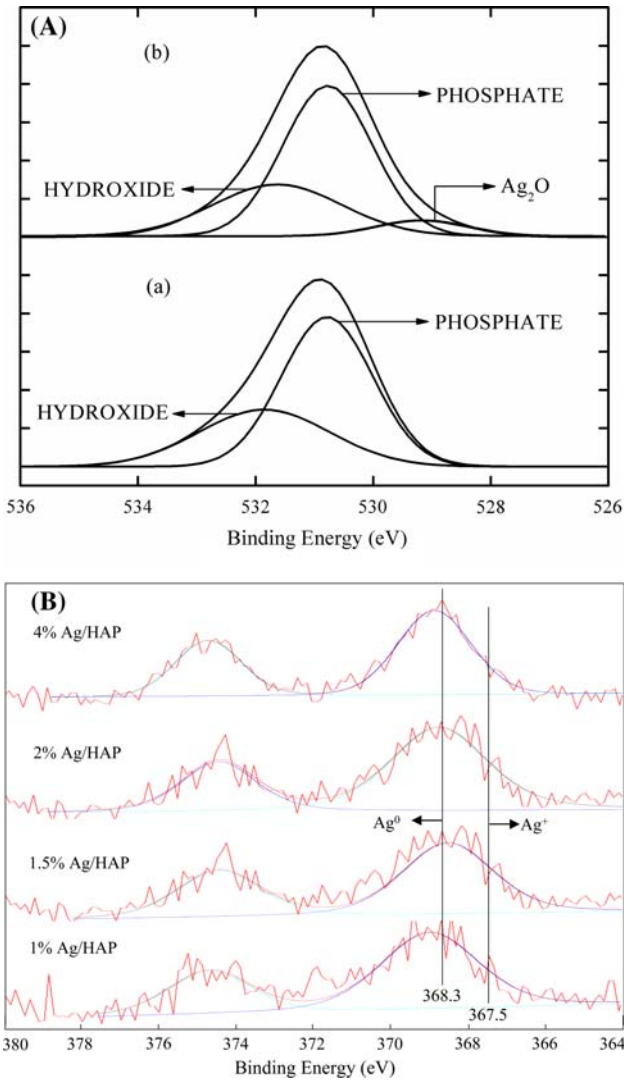

Fig. 3 XPS spectra of (**a**) O1 s: (a) HAp (b) 1.5% Ag/Hap catalysts. (**b**) Ag 3d: Ag (wt.%) loaded Hap catalysts

Table 3 TPR and TPD of NH_3 characteristics of HAp and Ag/HAp catalysts

Catalyst	H_2 uptake (μmol/g)	T_{max} (°C)	NH_3 desorbed (μmol/g)	T_{max} (°C)
Hydroxyapatite	0.0	–	55.4	126
0.5% Ag/HAp	10.5	210.5	48.2	110
1.0% Ag/HAp	38.4	203.6	44.7	94
1.5% Ag/HAp	48.2	179.5	39.6	94
2.0% Ag/HAp	37.5	182.6	30.8	91
4.0% Ag/HAp	35.2	167.7	29.5	100

consumptions at their corresponding T_{max} of reduction of all the catalysts are given. It can be seen from Fig. 4 that the T_{max} of the peak decreased from lower loadings to higher, which is assigned to the increase in size of Ag_2O clusters with loading (Table 1). The highest intensity and broad reduction peak is observed for 1.5 wt.% Ag/HAp among all the catalysts indicating that the well dispersed higher amount of small Ag_2O clusters (19 nm) are present over this catalyst in comparable amount of Ag loaded. Since 1.5 wt.% Ag/HAp catalyst showed the highest activity for NO_x conversion, this activity seems to be dependent on the amount of small Ag_2O clusters (19 nm) and dispersion. The maximum reduction peak of Ag_2O is observed at 179.5 °C for 1.5 wt.% Ag/HAp with high hydrogen consumption of 48.2 μmol [31]. Hydrogen consumptions increased with the increasing silver loading upto 1.5 wt.% Ag/HAp catalyst and then decreased, which suggests the presence of high amount silver oxide in lower loadings. In case of 2 and 4 wt.% Ag/HAp catalysts low temperature reduction may be attributed to the formation of high amount of metallic silver and bigger particles of silver oxide of 35 nm and 51 nm, which is also observed in XRD and XPS results.

3.4 Activity

Activity measurements are carried out with the reaction mixture containing 800 ppm NO_x, 800 ppm C_3H_6 and 6% O_2 balanced helium gas. Figures 5 and 6 show the NO_x conversions and the NO_x conversion to N_2. There is no formation of ammonia observed throughout the reaction temperatures from 250 to 500 °C. The pure hydroxyapatite was found to be poorly active for the NO_x reduction. Under the reaction conditions the vacancy formed on the surface of phosphate group of HAp transfers the electrons to Ag_2O to reduce the incoming NO_x by propene with redox mechanism at low temperatures [32, 33]. This may be due to the lattice oxygen participation from the phosphate group in HAp to increase conductivity of Ag, which is well reported over V_2O_5-WO_3/TiO_2 catalyst [34, 35]. The activity of the high silver loaded catalyst is significantly different from that of the hydroxyapatite and the lower loading catalysts. However, Ag/HAp catalysts with lower loadings of silver showed high temperature NO_x conversion and vice versa. The temperature range of NO_x conversion in presence of oxygen was explained for the Ag/HAP catalyst according to the proposed reaction

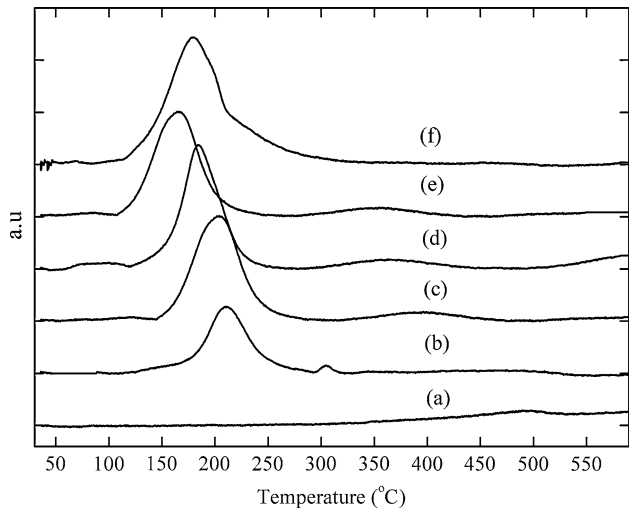

Fig. 4 H_2-TPR profiles of fresh catalysts (a) HAp (b) 0.5% Ag/Hap (c) 1% Ag/HAp (d) 2% Ag/HAp (e) 4% Ag/HAp (f) 1.5% Ag/Hap

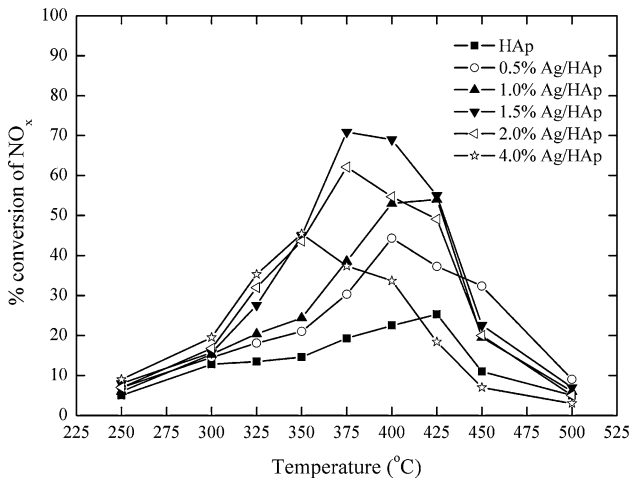

Fig. 5 NO_x conversion of HAp and Ag/HAp catalysts. Conditions: 800 ppm, NO_x, 800 ppm C_3H_6, 6% O_2, helium balance, total flow rate 100 cc/min, 0.25 g catalyst

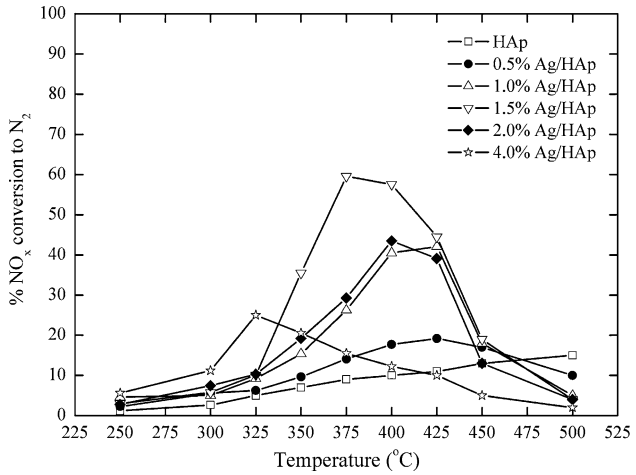

Fig. 6 NO_x conversion to N_2 of HAp and Ag/HAp catalysts. Conditions: 800 ppm NO_x, 800 ppm C_3H_6, 6% O_2, helium balance, total flow rate 100 cc/min, 0.25 g catalyst

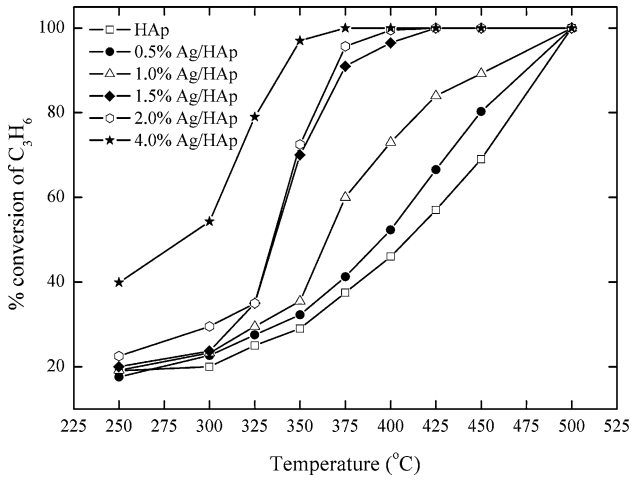

Fig. 7 Propene conversion of HAp and Ag/HAp catalysts. Conditions: 800 ppm NO_x, 800 ppm C_3H_6, 6% O_2, helium balance, total flow rate 100 cc/min, 0.25 g catalyst

scheme in Iwamoto et al. [36]. A maximum NO_x conversion of 45% is achieved at lower temperature at 350 °C over 4 wt.% Ag/HAp, where as with the decreasing Ag loading the temperature of maximum conversion increased. The 0.5 wt.% Ag/HAp yielded NO_x conversion at higher temperatures with lower NO_x to N_2 conversion. The NO_x to N_2 conversion over 1.5 wt.% Ag/HAp remained significantly higher than 1 and 2 wt.% Ag/HAp catalysts. The maximum NO_x conversion of 70% is achieved at low temperature 375 °C of 70% over 1.5 wt.% Ag/HAp with 60% NO_x to N_2 conversion due to the presence of well-dispersed Ag_2O prevailed by the phosphate group on HAp. H.-W. Jen [37] reported a lower NO_x to N_2 conversion of 40% observed at 400 °C temperatures over 2% Ag/Al_2O_3 catalyst. In case of 4 wt.% Ag/HAp catalyst the NO_x to N_2 conversion is very low, this may be due to higher silver loading and presence of larger metallic silver particles (Table 1), which lead to the non-selective reduction of NO_x and direct decomposition of the reductant. The maximum NO_x to N_2 conversion of 60% is obtained over 1.5 wt.% Ag/HAp at 375 °C and in 2 wt.% Ag/HAp of 44% at 400 °C. Whereas, in the case of 0.5 wt.% Ag/HAp catalysts 21% is achieved at 500 °C and over 4 wt.% Ag/HAp catalyst 25% conversion at 325 °C. In all cases, N_2 is the main product of reaction and N_2O is observed in small amounts.

Figure 7 shows propene conversion with temperature over HAp and Ag/HAp catalysts. The conversion profiles of hydrocarbon revealing that the partial oxidation of the hydrocarbon initiating the NO_x reduction and the complete oxidation at high temperatures is minimizing the availability of partially oxidized intermediates for the reduction of NO_x. Hence, the rate of the NO_x reduction may be decreasing [39]. Therefore, the temperature range for NO_x reduction is closely related to that for C_3H_6 oxidation as shown in Fig. 7. The complete conversion of the reductant is achieved at 375 °C over 4 wt.% Ag/HAp, in contrast to the temperatures of complete conversion over 0.5 wt.% Ag/HAp and HAp at 500 °C. The presence of bigger particles of metallic silver leads to low temperature decomposition of the propene in 4 wt.% Ag/HAp than over the catalysts with lower loadings of silver [39]. The complete conversion of propene is obtained at 500 °C for HAp, 0.5 and 1 wt.% Ag/HAp catalysts, whereas over 1.5, 2 and 4 wt.% Ag/HAp catalysts it is achieved at 425, 400 and 375 °C respectively. Further experiments are in progress to improve the activity of novel Ag/HAp catalyst by adding promoters.

4 Conclusions

In summary, increasing silver loading over HAp increased the NO_x conversion upto optimum level of silver (1.5%) and then decreased. The highest NO_x conversion of 70% is obtained over 1.5 wt.% Ag/HAp catalyst and also highest NO_x conversion to N_2 is observed at 375 °C. The higher performance of 1.5 wt.% Ag/HAp catalyst is due to presence of well-dispersed Ag_2O, which is observed in XRD, XPS and TPR results. Finally, it may be concluded that the presence of highly dispersed silver oxide in 1.5 wt.% Ag/HAp showed higher NO_x to N_2.

Acknowledgment This research work was supported by a grant (07K1501–01812) from 'Center for Nanostructured Materials Technology' under '21st Century Frontier R&D Programs' of the Ministry of Science and Technology, Korea.

References

1. Maunula T, Kintaichi Y, Inaba M, Haneda M, Sato K, Hamada H (1998) Appl Catal B: Environ 15:291
2. Ueda A, Oshima T, Haruta M (1997) Appl Catal B: Environ 12:81
3. Haneda M, Kintaichi Y, Shimada H, Hamada H (2000) J Catal 192:137
4. Shimizu K, Satsuma A, Hattori T (1998) Appl Catal B: Environ 16:319
5. Burch R, Breen JP, Meunier FC (2002) Appl Catal B: Environ 39:283
6. Burch R, Millington PJ, Walker AP (1994) Appl Catal B: Environ 4:65
7. Brooks TL (1981) Hydroxyapatite: calbiochem brand ciochemicals. San Diego, CA
8. Kibby CL, Lande SS, Hall WK (1972) J Am Chem Soc 94:214
9. Kibby CL, Hall WK (1973) J Catal 29:144
10. Sugiyama S, Minami T, Hayashi H, Tanaka M, Shigemoto N, Moffat JB (1996) J Chem Soc Faraday Trans 92:293
11. Sugiyama S, Shono T, Nitta E, Hayashi H (2001) Appl Catal A: Gen 211:123
12. Sebti S, Tahir R, Nazih R, Saber A, Boulaajaj S (2002) Appl Catal A: Gen 228:155
13. Sebti S, Tahir R, Nazih R, Boulaajaj S (2001) Appl Catal A: Gen 218:25
14. Zahouily M, Abrouki Y, Bahlaouan B, Rayadh A, Sebti S (2003) Catal Commun 4:521
15. Venugopal A, Scurrell MS (2003) Appl Catal A 245:137
16. Kaneda K, Mori K, Hara T, Mizugaki T, Ebitani K (2004) Catal Surv Asia 8:231
17. Miyadera T, Yoshida K (1993) Chem Lett: 1483
18. Meunier FC, Zuzaniuk V, Breen JP, Olsson M, Ross JRH (2000) Catal Today 59:287
19. She X, Flytzani-Stephanopoulos M (2006) J Catal 237:79
20. Bethke KA, Kung HH (1997) J Catal 172:93
21. He H, Zhang RD, Yu YB, Liu JF (2003) Chin J Catal 24:788
22. Delahay G, Coq B, Ensuque E, Figueras F (1996) Catal Lett 39:105
23. Haneda M, Kintaichi Y, Inaba M, Hamada H (1998) Catal Today 42:127
24. Satokawa S, Shibata J, Shimizu K, Satsuma A, Hattori T (2003) Appl Catal B: Environ 42:179
25. Meunier FC, Ukropec R, Stapleton C, Ross JRH (2001) Appl Catal B: Environ 30:163
26. Kundakovic L, Flytzani-Stephanopoulos M (1999) Appl Catal A: Gen 183:35
27. Martinez-Arias A, Fernandez-Garcia M, Iglesias-Juez A, Anderson JA, Conesa JC, Soria J (2000) Appl Catal B: Environ 28:29
28. Hayek E, Newesely H (1963) Inorg Synth 7:63
29. Bogdanchikova N, Meunier FC, Avalos-Borja M, Breen JP, Pestryakov A (2002) Appl Catal B: Environ 36:287
30. Moulder JF, Stickle WF, Sobol PE, Bomben KD (1992) Handbook of x-ray photoelectron spectroscopy. Perkin-Elmer, Eden Prairie
31. Furusawa T, Seshan K, Lercher JA, Lefferts L, Aika K (2002) Appl Catal B: Environ 37:205
32. Nishikawa H (2001) Mater Lett 50:364
33. Reddy MP, Venugopal A, Subrahmanyam M (2007) Water Res 41:379
34. Phil HH, Hyo JS, Sub LK, Ho HS (2006) Rare Metals 25:77
35. Lietti L, Forzatti P (1994) J Catal 147:241
36. Iwamoto M, Hamada H (1991) Catal Today 10:57
37. Jen H-W (1998) Catal Today 42:37
38. Zhang X, Yu Y, He H (2007) Appl Catal B: Environ 76:241
39. Li Z, Flytzani-Stephanopoulos M (1997) Appl Catal A: Gen 165:15